Surviving Granule Cells of the Sclerotic Human Hippocampus Have Reduced Ca^{2+} Influx Because of a Loss of Calbindin-D_{28k} in Temporal Lobe Epilepsy

U. Valentin Nägerl,[1] Istvan Mody,[1] Monika Jeub,[2] Ailing A. Lie,[2] Christian E. Elger,[2] and Heinz Beck[2]

[1]Department of Neurology and Physiology, University of California at Los Angeles School of Medicine, Los Angeles, California 90095, and [2]Department of Epileptology, University of Bonn Medical Center, D-53105 Bonn, Germany

In mesial temporal lobe epilepsy (mTLE), the predominant form of epilepsy in adults, and in animal models of the disease, there is a conspicuous loss of the intracellular Ca^{2+}-binding protein calbindin-D_{28k} (CB) from granule cells (GCs) of the dentate gyrus. The role of this protein in nerve cell function is controversial, but here we provide evidence for its role in controlling Ca^{2+} influx into human neurons. In patients with Ammon's horn sclerosis (AHS), the loss of CB from GCs markedly increased the Ca^{2+}-dependent inactivation of voltage-dependent Ca^{2+} currents (I_{Ca}), thereby diminishing Ca^{2+} influx during repetitive neuronal firing. Introducing purified CB into GCs restored Ca^{2+} current inactivation to levels observed in cells with normal CB content harvested from mTLE patients without AHS. Our data are consistent with the possibility of neuroprotection secondary to the CB loss. By limiting Ca^{2+} influx through an enhanced Ca^{2+}-dependent inactivation of voltage-dependent Ca^{2+} channels during prolonged neuronal discharges, the loss of CB may contribute to the resistance of surviving human granule cells in AHS.

Key words: Ammon's horn sclerosis; mesial temporal lobe epilepsy; granule cells; voltage-dependent Ca^{2+} currents; calcium channels; calbindin-D_{28k}

Ammon's horn sclerosis (AHS), present in approximately two-thirds of patients with mesial temporal lobe epilepsy (mTLE) (Blümcke et al., 1999), is characterized by a devastating loss of hippocampal neurons, comprising the hilus, and the CA1, CA3, and CA4 regions, whereas dentate gyrus granule cells (GCs) are conspicuously more resistant to the damage (Margerison and Corsellis, 1966; Blümcke et al., 1999). This selective loss of some, and sparing of other, neurons remains puzzling. Work on mTLE and animal models of limbic epilepsy has suggested that the neuronal damage may result from excessive and sustained epileptic seizures (Sagar and Oxbury, 1987; Meldrum, 1993; Wasterlain, 1997; Jackson et al., 1998). If frequent and prolonged seizures can kill nerve cells, then a likely mechanism for the ensuing neuronal loss is the activity-dependent accumulation of cytoplasmic Ca^{2+} entering the cells through voltage- and ligand-gated Ca^{2+}-permeable channels, or being released from intracellular stores (Miller, 1991; Ghosh and Greenberg, 1995; Berridge, 1998). Indeed, neurons tightly control the cytoplasmic concentration of free Ca^{2+} because it regulates critical cellular events ranging from signal transduction cascades and induction of gene transcription to neuronal death (Ghosh and Greenberg, 1995; Berridge, 1998).

Numerous cellular changes have been considered to be associated with AHS (Blümcke et al., 1999). Specific molecular events such as altered $GABA_A$ receptor subunits (Brooks-Kayal et al., 1998) or the loss of the neuronal Ca^{2+}-binding protein calbindin-D_{28k} (CB) (Baimbridge and Miller, 1984) occur even before the generalization of seizures. Of the known cellular changes, the loss of CB in the surviving dentate gyrus granule cells of human mTLE patients (Maglóczky et al., 1997), also present in several animal models of the disease (Miller and Baimbridge, 1983; Baimbridge and Miller, 1984; Baimbridge et al., 1985; Shetty and Turner, 1995; Yang et al., 1997), gives the closest clue to an altered Ca^{2+} homeostasis in these mTLE-affected neurons. The role of CB in nerve cells is not well understood (Baimbridge et al., 1992). Many reports (Sloviter, 1989; Lledo et al., 1992; Cheng et al., 1994) consider its presence in neurons to convey resistance against excessive Ca^{2+}-dependent neuronal damage. A contrasting view, based on recent findings in CB knock-out animals (CB−/−) (Klapstein et al., 1998) is that its absence may actually alleviate Ca^{2+}-dependent neuronal damage. The discovery of a Ca^{2+}-dependent promoter for CB (Arnold and Heintz, 1997), and the loss of CB from granule cells in several animal models of TLE (Miller and Baimbridge, 1983; Baimbridge and Miller, 1984; Köhr et al., 1991; Shetty and Turner, 1995; Yang et al., 1997) raises the possibility that levels of CB may be regulated in a Ca^{2+}-dependent manner subsequent to changes in neuronal excitability. In the kindling model, the CB loss has been suggested to serve a neuroprotective role, by limiting the amount of Ca^{2+} entry during prolonged action potential firing (Köhr and Mody, 1991). We directly addressed the regulation of Ca^{2+} entry into human hippocampal neurons that survived AHS associated with mTLE. A reduced Ca^{2+} entry, compared to that found in cells with no CB loss obtained from nonsclerotic hippocampi, would be

Received Oct. 7, 1999; revised Dec. 17, 1999; accepted Dec. 22, 1999.

This study was supported by an American Epilepsy Foundation predoctoral fellowship to U.V.N., National Institutes of Health/ National Institute of Neurological Disorders and Stroke (NINDS) Grant NS 36141 and the Coelho Endowment to I.M., and grants from BONFOR 111/2, SFB 400, and DFG EL 122/7–1 to H.B. and C.E.E. The human tissue was kindly provided by Dr. Itzak Fried (Division of Neurosurgery, UCLA School of Medicine) and Dr. Masako Isokawa (Brain Research Institute, UCLA School of Medicine), members of the NINDS Program Project "A Clinical Research Program for the Partial Epilepsies" (Dr. Jerome Engel Jr, Program Director, Department of Neurology, UCLA School of Medicine) and Drs. Schramm, Zentner, and van Roost (Department of Epileptology, University of Bonn Medical Center). We thank Dr. K. G. Baimbridge (Department of Physiology, University of British Columbia) for supplying recombinant human CB.

Correspondence should be addressed to Istvan Mody, Department of Neurology RNRC 3-155, UCLA School of Medicine, 710 Westwood Plaza, Los Angeles, CA 90095-1769. E-mail: mody@ucla.edu.

Table 1. Clinical data on epileptic patients

Code	Age and gender	Clinical history in addition to TLE	Duration	Seizure type	Diagnosis	No. of cells
A1	50 f	Perinatal hypoxia	48	SGS, CPS	AHS	4
A2	19 f	Complicated febrile seizure	14	SPS, CPS, SGS	AHS	1
A3	23 f	—	23	SPS, CPS	AHS	3
A4	42 m	Febrile seizures, meningitis	35	SPS, CPS	AHS	3
A5	19 f	Migraine, febrile seizures, mild hemiparesis	5	CPS, SGS	AHS	4
A6	32 f	Febrile seizures	32	SPS, CPS, SGS	AHS	4
A7	38 f	—	5	CPS, SGS	AHS	1
A8	42 m	IDDM, diabetic PNP, paranoid psychosis	34	CPS, SGS	AHS	1
A9	41 m	—	11	SPS, CPS, SGS	AHS	6
A10	38 m	Meningitis with febrile seizure	38	SPS, CPS, SGS	AHS	1
A11	32 m	Febrile seizure	24	CPS, SGS	AHS	4
A12	32 f	—	25	CPS, SGS	AHS	2
A13	22 f	Tuberculous meningitis	14	SPS, CPS, SGS	Postencephalitic scars	3
A14	42 f	—	8	CPS	AHS	5
A15	28 m	Multiple seizure disorders	9	CPS	Mild HS, cryptogenic	3
A16	52 f	Schizophrenia, psychosis	52	CPS	AHS	5
A17	49 f	—	43	CPS	AHS	2
L1	33 m	Pilocytic Astrocy-toma (WHO grade 1)	25	CPS, GMS	Multiple GNH	1
L2	37 m	Contusio cerebri (17 yrs)	19	CPS	Multiple glial scars	1
L3	10 m	One-sided spastic hemiparesis	2	CPS, SGS	Polymicro-gyria	1
L4	33 f	Partly resected angioma left temporal (22 y)	11	CPS	Arterio-venous malformation	3
L5	32 f	Proencephalic cyst, iron deficiency anaemia, hemiparesis	29	CPS, SGS	Glial scars	2
L6	42 m	Perinatal hypoxia	27	SPS, CPS, SGS	GNH	2
L7	25 f	—	14	SPS, CPS, SGS	Ganglio-glioma	1
L8	49 f	—	24	SPS, CPS	Dysembryoblastic neuroepithelial tumor	3

m, Male; f, female; IDDM, insulin-dependent diabetes mellitus; PNP, polyneuropathy; SPS, simple partial seizures; CPS, complex partial seizures; SGS, secondary generalized seizures; AHS, Ammon's horn sclerosis; GNH, glio-neuronal hamartia; HS, hippocampal sclerosis; TLE, temporal lobe epilepsy.

All subjects were adults and suffered from medically intractable epilepsy. Patients were grouped into two classes according to histopathological diagnosis of either Ammon's horn sclerosis (A) or a lesion (L) in the temporal lobe but not in the hippocampus proper.

consistent with the loss of CB and the ensuing diminished Ca^{2+} entry having saved the granule cells from devastation in AHS. The availability of recombinant CB made possible its infusion into the very neurons that lost it during the course of the disease, thus directly addressing its role in the control of neuronal Ca^{2+} entry. We have exploited the unique opportunities provided by our epilepsy surgery programs (Engel, 1993; Schwartzkroin, 1993) to perform concomitant morphological and physiological analyses on human hippocampi resected from mTLE patients.

MATERIALS AND METHODS

Patient subjects. All patients had therapy-refractory mTLE and were under a full antiepileptic drug regimen at the time of surgery (Engel, 1993). Clinical data were not significantly different between the AHS and the lesion group (Table 1). Hippocampal control specimens were obtained at autopsy from two individuals without any history of neurological or psychiatric disease (cause of death: respiratory insufficiency caused by severe pneumonia and cardiogenic shock caused by myocardial infarction, respectively). Informed consent was obtained from all patients for additional histopathological and electrophysiological evaluation. All procedures were approved by the respective ethics committees of the University of Bonn Medical Center and the UCLA Human Subject Protection (protocol HSPC no. 93-11-642-11) and conform to standards set by the Declaration of Helsinki (1989).

Immunohistochemistry and quantification of CB-immunoreactive GCs. Immunohistochemistry for CB was performed on 4-μm-thick paraffin-embedded sections of the hippocampi obtained from the patients whose cells were used for patch-clamp recordings. In addition, hippocampal control specimens were obtained at autopsy from two individuals without any history of neurological or psychiatric disease. All specimens were processed in a single batch according to standard methods. Specimens were stained with a primary antibody (1:1000; anti-calbindin-D_{28K}; Swant, Bellinzona, Switzerland) overnight at 4°C. Binding of the primary antibody was detected by the avidin—biotin–complex peroxidase method (ABC Elite; Vector Laboratories, Burlingame, CA), using 3,3′-diaminobenzidine (ICN Biochemicals, Cleveland, OH) as a chromogen. Sections were lightly counterstained with hematoxylin, dehydrated, and mounted. Control experiments with omission of primary antibodies, as well as substitution of the primary antibody by equivalent dilutions of nonimmune rabbit IgG serum (Dako, Glostrup, Denmark), showed no immunoreaction product. For quantitative analysis of CB immunoreactivity, sections were scanned at a magnification of 1000× using a Vanox microscope (Olympus, Tokyo, Japan), a CCD video camera (Sony, Tokyo, Japan), and the IP Lab imaging analysis software (Signal Analytics Corporation, Vienna, Austria) on a MacIntosh computer (7100/66; Apple). Optical densities (OD) were recorded as values on a gray scale ranging from 0 (black) to 255 (white) for 10 randomly selected GC bodies, each within three defined regions of interest (superior blade, inferior blade, and apex of the dentate gyrus) per specimen. ODs of the alveus devoid of immunoreaction product served as reference values. Within each specimen, ODs determined for the GC bodies were subtracted from the reference value.

Preparation of acutely isolated dentate granule cells. Isolated hippocampal granule cells were prepared as described previously (Beck et al., 1997a,b, 1999; Nägerl and Mody, 1998). Human hippocampal specimens were placed in ice-cold artificial CSF (ACSF) immediately after surgical removal. Coronal slices, 400-μm-thick, were prepared from the corpus of the hippocampus with a vibratome and transferred to a storage chamber with warmed (32°C) ACSF. After an equilibration period of 60 min, enzymatic digestion was performed for 25 min with 2–3 mg/ml pronase (protease type XIV; Sigma, St. Louis, MO). The dentate gyrus was dissected under a binocular microscope (Zeiss, Oberkochen, Germany)

and triturated in 2 ml of trituration solution with fire-polished glass pipettes. The cell suspension was then placed in a Petri dish for subsequent patch-clamp recordings. Only neurons with ovoid somata and a single dendrite reminiscent of granule cell morphology *in situ* were included in this study. The isolated cells were superfused with an extracellular solution containing (in mM): tetraethylammonium chloride (TEA) 140, 4-aminopyridine (4-AP) 5, $CaCl_2$ 5, glucose 10, and HEPES 10, and tetrodotoxin (TTX) 1 μM (chemicals obtained from Sigma and Fluka, Buchs, Switzerland). The osmolarity was adjusted to 283 mOsm with sucrose.

Patch-clamp whole-cell recording. Patch pipettes were made from borosilicate glass capillaries (outer diameter, 1.5 mm; inner diameter, 1 mm; Science Products, Hofheim, Germany or Garner Glass) with a resistance of 2–3 MΩ. The pipettes were filled with an intracellular solution containing (in mM): Cs-methanesulfonate 80, TEA 20, $MgCl_2$ 5, HEPES 10, ATP 10 and GTP 0.2, pH 7.4, CsOH. The osmolarity was adjusted to 275–280 mOsm with sucrose in all intracellular solutions. In some experiments, CB (500–1300 ng/μl) was included in the intracellular solution. For this purpose, lyophilized CB (Swant; Dr. K. G. Baimbridge, University of British Columbia) was reconstituted with bidistilled water, followed by buffer replacement with intracellular solution using Bio-Spin Chromatography Columns (Bio-Gel P-6; Bio-Rad, Munich, Germany) according to the supplier's recommendation. Homodimers of CB were not present in the intracellular solution, as demonstrated by subjecting 3 μg of CB (Swant) reconstituted in bidistilled water as well as 3 μg of CB purified by a Bio-Spin Chromatography Column (Bio-Rad) to 10% SDS-PAGE. Visualization of proteins on gels by Coomassie blue showed a single band at ~28 kDa (data not shown). For the recordings including CB in the intracellular solution, the tip of the electrode was dipped briefly (1 sec) into CB-free intracellular solution and back-filled with CB-containing solution. Recordings performed with different intracellular solutions were interleaved in individual patients to minimize effects caused by interpatient variability. Tight-seal whole-cell recordings were obtained at room temperature (21–24°C) (Beck et al., 1997a,b, 1999; Nägerl and Mody, 1998). Membrane currents were recorded using the EPC9 patch-clamp amplifier (Heka Elektronik, Lambrecht/Pfalz, Germany) and the TIDA acquisition and analysis program (HEKA Elektronik). To generate AP waveforms for voltage-clamp commands, a single action potential was recorded from GCs using an Axopatch 200B amplifier (Axon Instruments, Foster City, CA) in the fast current-clamp mode and the WinWCP Strathclyde Electrophysiology Software version 2.1 (courtesy of Dr. J. Dempster, University of Strathclyde). It was Bessel-filtered (8-pole) at 5 kHz, digitized at 20 kHz, and subsequently concatenated to produce a 1 sec 108 Hz AP train. The train was digital-to-analog-converted with an update rate of 10 kHz (PCI-MIO E16–4; National Instruments, Austin, TX) and applied as a voltage command. To minimize capacitive artifacts, all current traces were linear leak-subtracted according to the P/4 protocol (Bezanilla and Armstrong, 1977) or using the EPC9 leak subtraction protocol. Series resistance was compensated by 60–80%. The maximal residual voltage error estimated by multiplying the maximal Ca^{2+} current amplitude with the effective series resistance after compensation did not exceed 3 mV. A liquid junction potential of −9.7 mV was calculated between the intracellular and extracellular solution with the generalized Henderson liquid junction potential equation, as described (Barry and Lynch, 1991). This value was subtracted from V_h. All results were expressed as mean values ± SEM. Differences were proven with a Mann–Whitney *U* Wilcoxon rank test, with the significance level set to 0.05 and denoted with asterisks in the figures.

RESULTS

Distribution of CB in the hippocampi of mTLE patients

We have obtained hippocampal specimens for electrophysiological and morphological investigations from mTLE patients. The patients were divided into two distinct groups (see Table 1 for clinical patient data). The first group comprised patients with a histopathological diagnosis of AHS characterized by severe neuronal loss in the CA1, CA3, and CA4 subfields and relative sparing of CA2 and the dentate gyrus (AHS group; Margerison and Corsellis, 1966). In this group, most cells in the granule cell layer were devoid of CB immunoreactivity (Fig. 1*C*). The second group consisted of patients without AHS but with lesions in the temporal lobe (lesion group) that did not involve the hippocampus proper. In this group, GCs show a pattern of CB immunoreactivity comparable to that of control biopsy specimens stained under identical conditions (Fig. 1*A,B*). The cumulative probability plot (Fig. 1*D*) of the OD of the immunoreaction product from single GC bodies quantitatively illustrates this dichotomy in hippocampal CB content. The average density of the CB immunoreactivity over the cells was: AHS, 4.1 ± 1.2; lesion, 41.1 ± 9.3; and control, 56.5 ± 6.1.

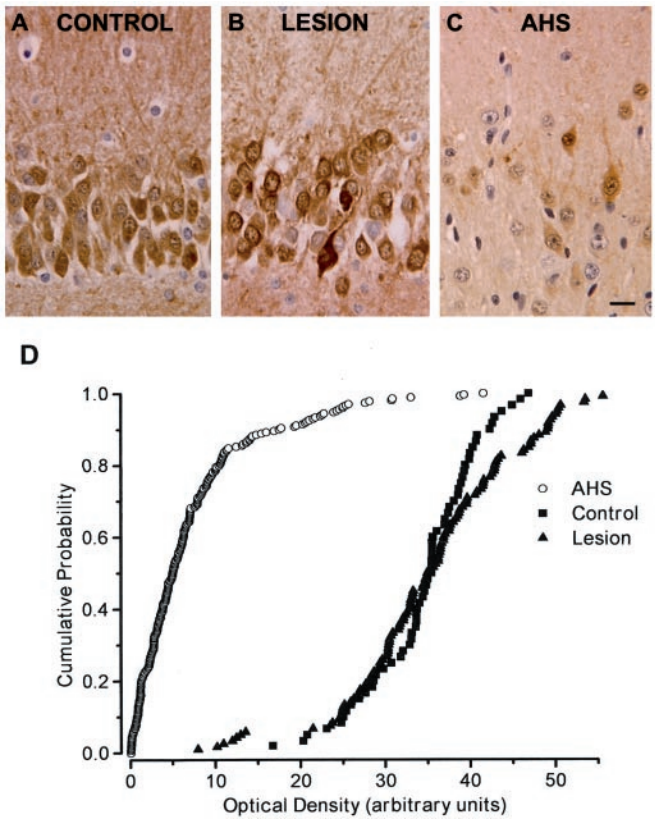

Figure 1. Immunohistochemistry for CB in dentate granule cells. All three photographs represent the granule cell layer with the granule cell bodies (stained dark for CB in *A* and *B*). Above the granule cells, the inner molecular layer is visible, whereas below the granule cell layer, part of the polymorphic cell layer of the dentate gyrus can be seen. *A,* In autopsy control hippocampi, the majority of dentate granule cells were intensely stained for CB. *B,* Specimens obtained from mTLE patients of the lesion group showed pronounced immunoreactivity in most dentate granule cells, corresponding well to the immunoreactivity pattern seen in the autopsy specimens. *C,* In contrast, AHS specimens displayed very faint or no CB immunoreactivity in the majority of dentate granule cells. Only a few neurons were immunopositive for CB. Sections are counterstained with hematoxylin. Scale bar, 10 μm. *D,* Cumulative probability plots of OD in hippocampal sections from autopsy control (*filled triangles*), lesion (*filled circles*), and AHS (*open circles*) patients as a measure for CB immunoreactivity. Each symbol represents the referenced OD for a single GC body.

Increased inactivation of I_{Ca} in human neurons lacking CB

Hippocampal specimens were obtained at surgery, and GCs were isolated according to standard protocols (Beck et al., 1996, 1997a, 1999; Nägerl and Mody, 1998). In parallel, the specimens were also classified based on CB immunohistochemistry. As a quantitative measure for the Ca^{2+}-dependent inactivation, we recorded voltage-dependent Ca^{2+} currents in the whole-cell configuration (Fig. 2*A*) using double-pulse experiments. A U-shaped relation-

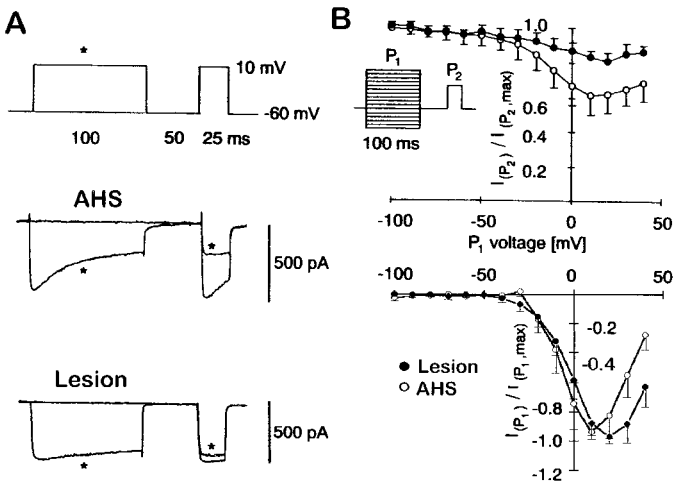

Figure 2. Ca^{2+}-dependent I_{Ca} inactivation as measured by double-pulse experiments. *A,* Representative traces illustrating the inactivation of Ca^{2+} currents evoked by P_2 after previous influx of Ca^{2+} during a 100 msec prepulse (P_1, marked by *asterisk*) in GCs isolated from a patient with AHS and a patient with lesion-associated epilepsy. Note the more rapid Ca^{2+} current inactivation during P_1 in patients with AHS. *B,* Peak current amplitudes during the test pulse (P_2) were normalized to their maximal amplitudes, averaged separately for the lesion group (*filled circles*; $n = 14$) and the AHS group (*open circles*; $n = 25$), and plotted versus the command voltage of the 100 msec prepulse. The *bottom panel* shows the normalized amplitudes of the Ca^{2+} current during the conditioning prepulse P_1.

ship between the command voltage of the conditioning prepulse (P_1; Fig. 2*B, inset*) and the I_{Ca} amplitude evoked by a test pulse (P_2) delivered 50 msec later is indicative of a Ca^{2+}-dependent I_{Ca} inactivation process. This amplitude directly measures the level of inactivation produced by previous Ca^{2+} entry (Eckert and Chad, 1984). Relating the peak amplitude of I_{Ca} evoked by single voltage pulses to the rate of its decay represents an alternative measure for the Ca^{2+} dependency of I_{Ca} inactivation, which we have used previously to characterize the enhanced I_{Ca} inactivation in GCs obtained from AHS mTLE patients (Nägerl and Mody, 1998; Beck et al., 1999). According to the double-pulse experiments, Ca^{2+}-dependent inactivation is considerably more pronounced in the AHS group (Fig. 2*A*), as measured by the ratios of the test pulse I_{Ca} amplitude and the peak I_{Ca} evoked by P_2. The minimal ratios were observed at +10 mV P_1 voltage for the AHS group (0.59 ± 0.08, $n = 25$) and at +20 mV for the lesion group (0.81 ± 0.07, $n = 14$, $p < 0.005$; Fig. 2*B*). The decay time constants of the I_{Ca} in the three experimental conditions were (in msec): AHS, 52.7 ± 5.5; lesion, 172.6 ± 94; and AHS + CB, 146.2 ± 73.6.

We used nifedipine to estimate the contribution of L-type Ca^{2+} channels to the whole-cell I_{Ca} inactivation. Bath application of nifedipine blocked up to $45.1 \pm 3.7\%$ ($n = 4$) of the I_{Ca} amplitude and diminished inactivation in AHS GCs from a ratio of 0.59 ± 0.08 ($n = 25$) to 0.88 ± 0.12 ($n = 4$) (data not shown). This indicates that most of the observed inactivation can be ascribed to L-type Ca^{2+} channels and that >75% of the L-type current inactivates after a 100 msec depolarization.

I_{Ca} inactivation after infusion of purified CB into AHS neurons devoid of CB

Next, we tested whether introduction of purified CB into granule cells of patients with AHS restores the Ca^{2+}-dependent inactivation to levels seen in the lesion group. Indeed, inclusion of 500 ng/μl (~20 μM) of purified CB into the intracellular solution (Fig. 3*A, bottom panel*) substantially reduced Ca^{2+}-dependent inactivation measured by double-pulse protocols compared to recordings without CB obtained in a GC from the same patient (Fig. 3*B, top panel*). Figure 3*C* demonstrates the effect of CB on I_{Ca} in a single cell as CB gradually diffuses into the cell after patch rupture. Recordings with ($n = 6$) and without ($n = 7$) CB were alternated to ensure that the effects of CB were not caused by interpatient variability. When the normalized ratios of Ca^{2+} current amplitudes during P_2 were averaged, the presence of purified CB in the patch pipette considerably reduced the inactivation (0.75 ± 0.05, $n = 6$) compared to the corresponding recordings without CB (0.57 ± 0.05, $n = 7$; Fig. 3*D*). This effect

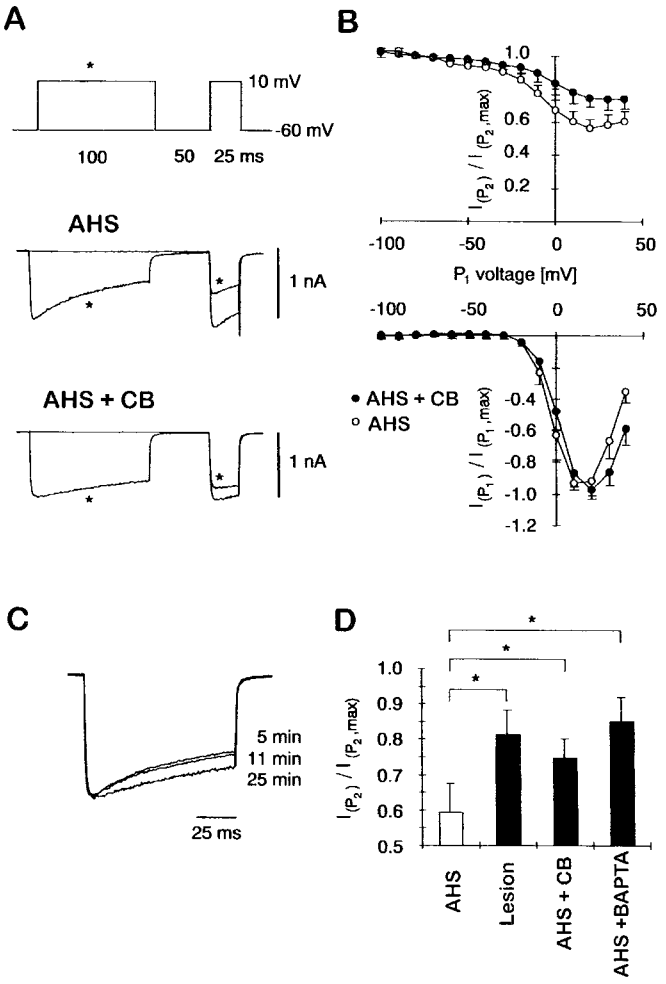

Figure 3. The effect of 500 ng/μl (~20 μM) CB infused into GCs lacking CB that were obtained from patients with AHS. *A,* Representative traces illustrating Ca^{2+}-dependent inactivation of Ca^{2+} currents in GCs from patients with AHS with and without purified CB included in the intracellular solution. Note that the Ca^{2+} current inactivation becomes slower after the intracellular dialysis of CB. *B,* Ca^{2+}-dependent inactivation was measured as in Figure 2*B*. Averages of three neurons treated with CB (*gray circles*) and four neurons without CB (*open circles*) from one individual patient are shown. *C,* Time course of the effect of intracellular dialysis of CB into one GC on I_{Ca} inactivation at 5, 11, and 25 min after patch rupture. *D,* Bar graph showing the minimal ratios as calculated in Figure 2*B* for the four experimental conditions: AHS ($n = 32$), lesion ($n = 14$), AHS + CB ($n = 6$), and AHS + BAPTA (5 mM, $n = 5$). Recordings with different intracellular solutions were interleaved to minimize interpatient variability. *Asterisks* indicate significant differences (Mann–Whitney *U* Wilcoxon rank test, $p < 0.05$).

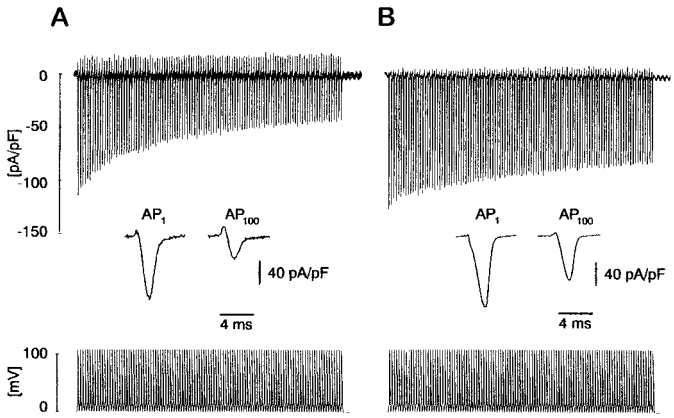

Figure 4. Ca^{2+} entry during action potential trains is reduced in the absence of CB. *A,* Representative Ca^{2+} currents evoked by a 1 sec train of action potential waveforms at 108 Hz are shown. In CB-deficient GCs the total amount of Ca^{2+} entry per AP waveform decreases from the first (AP_1) to the last AP (AP_{100}) by ~75% (see *inset*). *B,* Reintroduction of 1300 ng/μl (~50 μM) purified CB into GCs via the patch pipette prevents the decrease of total Ca^{2+} entry during an AP train. The difference in integrated charge between the last AP and the first is only ~50% (see *inset*).

of CB was comparable to those obtained with including the synthetic Ca^{2+} buffer BAPTA (5 mM; inactivation ratio 0.85 ± 0.07, $n = 5$) into the patch pipette.

CB controls the Ca^{2+} entry induced by a train of action potentials

Using trains of action potential (AP) waveforms in the whole-cell voltage-clamp mode, we mimicked physiological Ca^{2+} entry during high-frequency neuronal firing to probe possible functional consequences of the CB-dependent Ca^{2+} current inactivation in mTLE GCs. Intracellular CB perfusion via the patch pipette into GCs from AHS patients gradually slowed the rate of decay of the Ca^{2+} entry evoked by AP trains. To quantify the AP-dependent Ca^{2+} entry, the I_{Ca} associated with the last and the first AP in the train were integrated to calculate the total charge. The respective charge ratios were taken as a measure of the effect of CB on spike train-induced Ca^{2+} entry. As shown in Figure 4*B,* the charge ratio of a 1 sec 108 Hz train is significantly increased to 0.50 ± 0.02 ($n = 4$; $p < 0.005$) in AHS GCs after CB infusion (1300 ng/μl at 50 μM) from 0.37 ± 0.02 ($n = 4$) in CB-deficient GCs (Fig. 4*A*), whereas the total charge associated with the first AP of the train did not differ under the two conditions (0.191 ± 0.006 mC/F with CB, 0.195 ± 0.036 mC/F without CB, total charge normalized to cell capacitance). The infusion of the synthetic Ca^{2+} chelator BAPTA (5 mM) instead of CB also increased the charge ratio to 0.52 ± 0.03 ($n = 5$; $p < 0.005$ compared to AHS GCs), an effect indistinguishable from that of CB.

DISCUSSION

We have shown that by controlling the Ca^{2+}-dependent inactivation of the high-voltage-activated L-type Ca^{2+} current, CB can regulate the amount of Ca^{2+} entry into human epileptic CNS neurons. Two mTLE patient groups identified on the basis of hippocampal cell loss also diverged with regard to the CB content of dentate gyrus granule cells. These two patient groups provided us with the opportunity to record from human neurons with reduced and normal CB levels. The group with severe hippocampal cell loss (AHS) showed a marked reduction in granule cell CB levels (Maglóczky et al., 1997), an enhanced Ca^{2+} current inactivation (Nägerl and Mody, 1998; Beck et al., 1999), and a reduced Ca^{2+} entry after repetitive firing. Granule cells in nonsclerotic hippocampi (lesion group) displayed normal levels of CB and moderate Ca^{2+} current inactivation. A similar correlation of CB loss in GCs and altered Ca^{2+} current inactivation is found in an experimental animal model of TLE (kindling; Köhr and Mody, 1991; Köhr et al., 1991). We have now demonstrated the involvement of CB in altered Ca^{2+} current inactivation, because the reduced Ca^{2+} entry in AHS granule cells could be reversed by directly introducing CB into the neurons.

The Ca^{2+}-dependent inactivation of voltage-gated Ca^{2+} channels is a key factor in limiting neuronal Ca^{2+} entry. If CB is to play an active role in the control of this process, it must either interact directly with the channel or it has to reach sufficiently high levels around the point $Ca^{2+}$of entry to effectively buffer the entering Ca^{2+} ions. Interestingly, the Ca^{2+}-binding protein calmodulin was recently shown to be the Ca^{2+} sensor responsible for inactivation (Lee et al., 1999; Levitan, 1999; Qin et al., 1999; Zuhlke et al., 1999). Because both CB and calmodulin bind Ca^{2+} to EF hand structures with possibly similar kinetics and affinities, it is conceivable that the estimated cytoplasmic CB concentrations of ~100 μM (Baimbridge et al., 1992) are normally sufficient to disrupt the negative Ca^{2+} feedback on the channel. However, the relatively low concentrations of infused CB sufficient in our experiments to restore the inactivation of Ca^{2+} are consistent with a close physical association or even an interaction between CB and the Ca^{2+} channels. Another EF-hand Ca^{2+}-binding protein, sorcin, has been shown to tightly associate with the α1 subunits of the cardiac and sarcoplasmic L-type Ca^{2+} channels (Meyers et al., 1998). At this time, there is no evidence for a similar association between CB any Ca^{2+} channel subunit, but recent evidence indicates a considerable fraction of CB to be found in the plasma membrane (Winsky and Kuznicki, 1995).

Regardless of the manner how CB controls the inactivation of Ca^{2+} entry through voltage-gated Ca^{2+} channels, the critical question is whether the loss of CB can lead to neuroprotection. Albeit counterintuitive, such an idea is consistent with the enhanced neuroprotection after ischemic insults in CB−/− mice (Klapstein et al., 1998). In addition to the Ca^{2+} dependent inactivation of Ca^{2+} channels, some of the cellular mechanisms involved in neuroprotection in the CB−/− mice may include enhanced activation of Ca^{2+} dependent K^+ channels and changes in synaptic facilitation. Nevertheless, most Ca^{2+} entry into neurons takes place when voltage-gated Ca^{2+} channels open during APs. Repetitive AP firing such as that occurring during seizures may thus exacerbate Ca^{2+} entry unless there is a Ca^{2+}-dependent negative feedback. Our experiments using action potential waveforms have shown that even at high frequencies, the first few action potentials in the train will produce comparable Ca^{2+} entry regardless of the presence or absence of CB. But in CB-deficient cells, the reduced Ca^{2+} entry during action potentials at the end of the train may be viewed as a use-dependent block of Ca^{2+} influx, turning to be gradually more pronounced as the duration of neuronal firing gets longer or its frequency becomes higher. If vulnerable neurons in AHS die directly from an excessive Ca^{2+} entry caused by prolonged high-frequency activity during seizures, then the protective mechanism against large Ca^{2+} loads provided by the loss of CB may indeed be responsible for the preservation of granule cells. Conversely, one would predict that granule cells that did not lose CB would be more prone to cell death in AHS patients. Yet, Maglóczky et al. (1997) did not report any differences at the EM level between CB-

deficient and CB-containing GCs. Nevertheless, the timing or mechanism of cell death in CB-positive neurons in AHS may preclude the identification of the neurodegenerative process in ultrastructural studies.

Presently, it is unknown what mechanisms control the decrease of CB levels in AHS but not in lesion-associated epilepsy. In neurons, the synthesis of CB is not vitamin D-dependent like in the periphery (Baimbridge et al., 1992), but the CB gene has a Ca^{2+}-dependent promoter (Arnold and Heintz, 1997) that may regulate CB synthesis, depending on the amount of neuronal activity. Interestingly, the only study examining the levels of CB mRNA when protein levels were clearly reduced in kindled animals found no change in the amount of message (Sonnenberg et al., 1991). This lack of change in CB mRNA in kindling raises the possibility of an enhanced activity-dependent degradation of CB.

Our findings also show that in spite of the protection of GCs against neuronal injury in AHS, the loss of granule cell CB did not prevent mTLE. In the future, the impact of the CB loss from GCs on the function of the dentate gyrus will have to be considered in the context of the entire hippocampal network. Nevertheless, for the first time in adult human neurons, we have directly demonstrated the role of CB in regulating Ca^{2+} influx in surviving cells of the sclerotic hippocampus. Thus, our findings demonstrate a strong link between cellular CB levels and the intracellular Ca^{2+} homeostasis, providing further insight into the relationship between cellular CB content and neuronal vulnerability.

REFERENCES

Arnold DB, Heintz N (1997) A calcium responsive element that regulates expression of two calcium binding proteins in Purkinje cells. Proc Natl Acad Sci USA 94:8842–8847.

Baimbridge KG, Celio MR, Rogers JH (1992) Calcium-binding proteins in the nervous system. Trends Neurosci 15:303–308.

Baimbridge KG, Miller JJ (1984) Hippocampal calcium-binding protein during commissural kindling-induced epileptogenesis: progressive decline and effects of anticonvulsants. Brain Res 324:85–90.

Baimbridge KG, Mody I, Miller JJ (1985) Reduction of rat hippocampal calcium-binding protein following commissural, amygdala, septal, perforant path, and olfactory bulb kindling. Epilepsia 26:460–465.

Barry PH, Lynch JW (1991) Liquid junction potentials and small cell effects in patch-clamp analysis. J Membr Biol 121:101–117.

Beck H, Blümcke I, Kral T, Clusmann H, Schramm J, Wiestler OD, Heinemann U, Elger CE (1996) Properties of a delayed rectifier potassium current in dentate granule cells isolated from the hippocampus of patients with chronic temporal lobe epilepsy. Epilepsia 37:892–901.

Beck H, Steffens R, Heinemann U, Elger CE (1997a) Properties of voltage-activated Ca^{2+} currents in acutely isolated human hippocampal granule cells. J Neurophysiol 77:1526–1537.

Beck H, Clusmann H, Kral T, Schramm J, Heinemann U, Elger CE (1997b) Potassium currents in acutely isolated human hippocampal dentate granule cells. J Physiol (Lond) 498:73–85.

Beck H, Steffens R, Heinemann U, Elger CE (1999) Ca^{2+}-dependent inactivation of high-threshold Ca^{2+} currents in hippocampal granule cells of patients with chronic temporal lobe epilepsy. J Neurophysiol 82:946–954.

Berridge MJ (1998) Neuronal calcium signaling. Neuron 21:13–26.

Bezanilla F, Armstrong CM (1977) Inactivation of the sodium channel. I. Sodium current experiments. J Gen Physiol 70:549–566.

Blümcke I, Beck H, Lie AA, Wiestler OD (1999) Molecular neuropathology of human mesial temporal lobe epilepsy. Epilepsy Res 36:205–223.

Brooks-Kayal AR, Shumate MD, Jin H, Rikhter TY, Coulter DA (1998) Selective changes in single cell GABA(A) receptor subunit expression and function in temporal lobe epilepsy. Nat Med 4:1166–1172.

Cheng B, Christakos S, Mattson MP (1994) Tumor necrosis factors protect neurons against metabolic-excitotoxic insults and promote maintenance of calcium homeostasis. Neuron 12:139–153.

Eckert R, Chad JE (1984) Inactivation of Ca channels. Prog Biophys Mol Biol 44:215–267.

Engel Jr J (1993) Surgical treatment of the epilepsies. New York: Raven.

Ghosh A, Greenberg ME (1995) Calcium signaling in neurons: molecular mechanisms and cellular consequences. Science 268:239–247.

Jackson GD, McIntosh AM, Briellmann RS, Berkovic SF (1998) Hippocampal sclerosis studied in identical twins. Neurology 51:78–84.

Klapstein GJ, Vietla S, Lieberman DN, Gray PA, Airaksinen MS, Thoenen H, Meyer M, Mody I (1998) Calbindin-D_{28k} fails to protect hippocampal neurons against ischemia in spite of its cytoplasmic calcium buffering properties: evidence from calbindin-D_{28k} knockout mice. Neuroscience 85:361–373.

Köhr G, Mody I (1991) Endogenous intracellular calcium buffering and the activation/inactivation of HVA calcium currents in rat dentate gyrus granule cells. J Gen Physiol 98:941–967.

Köhr G, Lambert CE, Mody I (1991) Calbindin-D_{28K} (CaBP) levels and calcium currents in acutely dissociated epileptic neurons. Exp Brain Res 85:543–551.

Lee A, Wong ST, Gallagher D, Li B, Storm DR, Scheuer T, Catterall WA (1999) Ca^{2+}/calmodulin binds to and modulates P/Q-type calcium channels. Nature 399:155–159.

Levitan IB (1999) It is calmodulin after all! Mediator of the calcium modulation of multiple ion channels. Neuron 22:645–648.

Lledo PM, Somasundaram B, Morton AJ, Emson PC, Mason WT (1992) Stable transfection of calbindin-D_{28k} into the GH3 cell line alters calcium currents and intracellular calcium homeostasis. Neuron 9:943–954.

Maglóczky Z, Halász P, Vajda J, Czirják S, Freund TF (1997) Loss of calbindin-D_{28k} immunoreactivity from dentate granule cells in human temporal lobe epilepsy. Neuroscience 76:377–385.

Margerison JH, Corsellis JA (1966) Epilepsy and the temporal lobes. A clinical, electroencephalographic and neuropathological study of the brain in epilepsy, with particular reference to the temporal lobes. Brain 89:499–530.

Meldrum BS (1993) Excitotoxicity and selective neuronal loss in epilepsy. Brain Pathol 3:405–412.

Meyers MB, Puri TS, Chien AJ, Gao T, Hsu PH, Hosey MM, Fishman GI (1998) Sorcin associates with the pore-forming subunit of voltage-dependent L-type Ca^{2+} channels. J Biol Chem 273:18930–18935.

Miller JJ, Baimbridge KG (1983) Biochemical and immunohistochemical correlates of kindling- induced epilepsy: role of calcium binding protein. Brain Res 278:322–326.

Miller RJ (1991) The control of neuronal Ca^{2+} homeostasis. Prog Neurobiol 37:255–285.

Nägerl UV, Mody I (1998) Calcium-dependent inactivation of high-threshold calcium currents in human dentate gyrus granule cells. J Physiol (Lond) 509:39–45.

Qin N, Olcese R, Bransby M, Lin T, Birnbaumer L (1999) Ca^{2+}-induced inhibition of the cardiac Ca^{2+} channel depends on calmodulin. Proc Natl Acad Sci USA 96:2435–2438.

Sagar HJ, Oxbury JM (1987) Hippocampal neuron loss in temporal lobe epilepsy: correlation with early childhood convulsions. Ann Neurol 22:334–340.

Schwartzkroin PA (1993) Basic research in the setting of an epilepsy surgery center. In: Surgical treatment of the epilepsies (Engel Jr J, ed), pp 755–773. New York: Raven.

Shetty AK, Turner DA (1995) Intracerebroventricular kainic acid administration in adult rat alters hippocampal calbindin and non-phosphorylated neurofilament expression. J Comp Neurol 363:581–599.

Sloviter RS (1989) Calcium-binding protein (calbindin-D_{28k}) and parvalbumin immunocytochemistry: localization in the rat hippocampus with specific reference to the selective vulnerability of hippocampal neurons to seizure activity. J Comp Neurol 280:183–196.

Sonnenberg JL, Frantz GD, Lee S, Heick A, Chu C, Tobin AJ, Christakos S (1991) Calcium binding protein (calbindin-D_{28k}) and glutamate decarboxylase gene expression after kindling induced seizures. Brain Res Mol Brain Res 9:179–190.

Wasterlain CG (1997) Recurrent seizures in the developing brain are harmful. Epilepsia 38:728–734.

Winsky L, Kuznicki J (1995) Distribution of calretinin, calbindin D_{28k}, and parvalbumin in subcellular fractions of rat cerebellum: effects of calcium. J Neurochem 65:381–388.

Yang Q, Wang S, Hamberger A, Celio MR, Haglid KG (1997) Delayed decrease of calbindin immunoreactivity in the granule cell- mossy fibers after kainic acid-induced seizures. Brain Res Bull 43:551–559.

Zuhlke RD, Pitt GS, Deisseroth K, Tsien RW, Reuter H (1999) Calmodulin supports both inactivation and facilitation of L-type calcium channels. Nature 399:159–162.